ANTIMICROBIAL AGENTS AND CHEMOTHERAPY, Jan. 2005, p. 249–255 Vol. 49, No. 1
0066-4804/05/$08.00+0 doi:10.1128/AAC.49.1.249–255.2005
Copyright © 2005, American Society for Microbiology. All Rights Reserved.

Antisense Phosphorodiamidate Morpholino Oligomer Length and Target Position Effects on Gene-Specific Inhibition in *Escherichia coli*

Jesse Deere,[1] Pat Iversen,[1] and Bruce L. Geller[1,2]*

AVI BioPharma[1] and Department of Microbiology,[2] Oregon State University, Corvallis, Oregon

Received 17 May 2004/Returned for modification 9 August 2004/Accepted 20 September 2004

Phosphorodiamidate morpholino oligomers (PMOs) are synthetic DNA analogs that inhibit gene expression in a sequence-dependent manner. PMOs of various lengths (7 to 20 bases) were tested for inhibition of luciferase expression in *Escherichia coli*. Shorter PMOs generally inhibited luciferase greater than longer PMOs. Conversely, in bacterial cell-free protein synthesis reactions, longer PMOs inhibited equally or more than shorter PMOs. Overlapping, isometric (10-base) PMOs complementary to the region around the start codon of luciferase inhibited to different extents in bacterial cell-free protein expression reactions. Including the anti-start codon in PMOs was not required for maximal inhibition. PMOs targeted to 5′ nontranslated or 3′ coding regions within luciferase mRNA did not inhibit, except for one PMO targeted to the ribosome-binding site. Inhibition of luciferase expression correlated negatively with the predicted secondary structure of mRNA regions targeted by PMO but did not correlate with C+G content of targeted regions. The effects of PMO length and position were corroborated by using PMOs (6 to 20 bases) targeted to *acpP*, a gene required for viability. Because inhibition by PMOs of ~11 bases was unexpected based on previous results in eukaryotes, we tested an 11-base PMO in HeLa cells and reticulocyte cell-free protein synthesis reactions. The 11-base PMO significantly inhibited luciferase expression in HeLa cells, although less than did a 20-base PMO. In reticulocyte cell-free reactions, there was a trend toward more inhibition with longer PMOs. These studies indicate that strategies for designing PMOs are substantially different for prokaryotic than eukaryotic targets.

Antisense drugs are short (10 to 25 bases) oligomers that mimic DNA or RNA and inhibit gene expression in a sequence-dependent manner (2, 6, 29, 30). They differ from native RNA or DNA in the chemical structure that links the four common bases.

Most of the reported work on antisense drugs has been accomplished in eukaryotic systems. In eukaryotes, antisense compounds inhibit by two general mechanisms. Compounds such as phosphorothioates hybridize to mRNA and promote its degradation by RNase H (3, 5, 28). Other compounds, such as peptide nucleic acid (PNA) and phosphorodiamidate morpholino oligomer (PMO), hybridize to specific mRNA and block translation by an RNase H-independent mechanism (3, 28).

The most effective region for targeting PNA and PMO is the 5′ untranslated region and initiation codon of mRNA (3, 10, 14, 15, 18, 20, 28, 30, 32). The optimal length of a PNA or PMO depends on achieving a balance between specificity and efficacy and is estimated to be about 15 to 25 bases (2, 14, 16, 21, 30). However, experimental evidence suggests that many factors, such as cellular uptake or invasion of mRNA secondary structure, influence efficacy and can tip the balance in favor of shorter antisense oligomers (13, 15, 19, 23, 31).

Sequence-specific antibacterial drugs are a recent application of antisense technology (11, 12, 17, 24, 25, 33). Nielsen and coworkers (13) have shown that PNA in the 9- to 12-mer range were more active inhibitors than larger oligomers in *Escherichia coli*. Antibacterial PNA targeted to the region near the AUG start codon inhibit their specific targets (12). A recent, systematic study with PNA showed that the region around the start codon is the most reliable target site for bacterial antisense inhibition (7). One objective of our studies was to compare and contrast the effects of PMO with that of PNA on the inhibition of gene expression in *E. coli*.

We show here the effects of varying the length and position of PMO on bacterial gene expression. Our results suggest differences between the mechanisms of antisense oligomer inhibition in bacteria compared to eukaryotic cells and between the effects of PMO and PNA on bacterial gene expression.

MATERIALS AND METHODS

PMOs. PMOs were synthesized and purified at AVI BioPharma, Inc. (Corvallis, Oreg.), as previously described (11), dissolved in water, filtered through a 0.2-μm-pore-size membrane (HT Tuffryn; Gelman Sciences, Inc., Ann Arbor, Mich.), and stored at 4°C. Sequences of PMOs used in the present study are shown in Table 1. The concentration of PMO was determined spectrophotometrically by measuring the absorbance at 260 nm and calculating the molarity by using an extinction coefficient calculated as described previously (4). The base sequences of nonsense PMOs were chosen randomly from a pool of bases that approximated the relative abundance of bases in the corresponding PMOs that were targeted to either *myc-luc* or *acpP*.

Bacteria and growth conditions. *E. coli* AS19 (26) and SM101 (9), which have defects in lipopolysaccharide synthesis that result in outer membrane permeability to high-molecular-weight solutes, were grown aerobically in Luria-Bertani broth at 37 and 30°C, respectively. Transformants that expressed pSE380myc-luc were grown in Luria-Bertani medium plus 100 μg of ampicillin/ml.

Reporter gene. Standard molecular biology procedures (1) were used for all constructions. All constructs were sequenced. Two reporter systems (pT7myc-luc and pSE380myc-luc) for antisense inhibition were previously constructed, as described previously (11), by fusing 30 bp of the 5′ end of human c-*myc* to all but

* Corresponding author. Mailing address: Department of Microbiology, Nash Hall 220, Oregon State University, Corvallis, OR 97331-3804. Phone: (541) 737-1845. Fax: (541) 737-0496. E-mail: gellerb@orst.edu.

TABLE 1. PMO characteristics

PMO	Target	Sequence (5′→3′)[a]	Length (no. of bases)	%G+C	2° score[b]
328	*myc-luc*	ACG TTG A	7	43	0
327	*myc-luc*	ACG TTG AG	8	50	0
326	*myc-luc*	ACG TTG AGG	9	56	0
208	*myc-luc*	ACG TTG AGG G	10	60	0
340	*myc-luc*	ACG TTG AGG GG	11	64	0
298	*myc-luc*	ACG TTG AGG GG**C**	12	67	0
250	*myc-luc*	ACG TTG AGG GG**C A**	13	62	0
249	*myc-luc*	ACG TTG AGG GG**C AT**	14	57	0
248	*myc-luc*	ACG TTG AGG GG**C AT**C	15	60	0
247	*myc-luc*	ACG TTG AGG GGC ATC G	16	62	0.0625
246	*myc-luc*	ACG TTG AGG GGC ATC GT	17	59	0.1176
245	*myc-luc*	ACG TTG AGG GGC ATC GTC	18	61	0.1667
126	*myc-luc*	ACG TTG AGG GGC ATC GTC GC	20	65	0.2000
239	*myc-luc*	G TTG AGG GGC ATC GTC GC	18	67	0.2222
240	*myc-luc*	TTG AGG GGC ATC GTC GC	17	65	0.2353
241	*myc-luc*	TG AGG GGC ATC GTC GC	16	69	0.2500
242	*myc-luc*	G AGG GGC ATC GTC GC	15	73	0.2667
243	*myc-luc*	AGG GGC ATC GTC GC	14	71	0.2857
244	*myc-luc*	GG GGC ATC GTC GC	13	77	0.3077
329	*myc-luc*	G GGC ATC GTC GC	12	75	0.3333
330	*myc-luc*	GGC ATC GTC GC	11	73	0.3636
331	*myc-luc*	GC ATC GTC GC	10	70	0.4000
332	*myc-luc*	C ATC GTC GC	9	67	0.4444
333	*myc-luc*	ATC GTC GC	8	62	NC
334	*myc-luc*	TC GTC GC	7	71	NC
341	*myc-luc* 5′ end transcript	GGA AAC CGT TGT GGT CTC CC	20	60	0.7500
342	*myc-luc* 5′ end transcript	AC CGT TGT GGT CTC CC	16	62	0.6875
343	*myc-luc* 5′ end transcript	GT TGT GGT CTC CC	13	69	0.6154
344	*myc-luc* 5′ end transcript	GT GGT CTC CC	10	70	0.8000
345	*myc-luc* RBS and 3′ of RBS	CGT CGC GGG ATT CCT TCT	18	61	0.3889
346	*myc-luc* 5′ of RBS	AAA GTT AAA CAA AAT TAT	18	11	0.1667
347	*myc-luc* RBS and 5′ of RBS	TCC TTC TTA AAG TTA AAC	18	28	0.3333
356	*myc-luc*	CGT TGA GGG G	10	70	0
357	*myc-luc*	GT TGA GGG G**C**	10	70	0
358	*myc-luc*	T TGA GGG G**CA**	10	60	0
359	*myc-luc*	TGA GGG G**CA T**	10	60	0
360	*myc-luc*	GA GGG G**CA T**C	10	70	0
361	*myc-luc*	A GGG GCA TCG	10	70	0.1000
362	*myc-luc*	GGG GCA TCG T	10	70	0.2000
363	*myc-luc*	GG GCA TCG TC	10	70	0.3000
364	*myc-luc*	G GCA TCG TCG	10	70	0.4000
214	*luc*, unpaired loop	AAT AGG GTT GG	11	45	0
215	*luc*, base-paired stem	TTT GCA ACC CC	11	55	0.9091
143	Nonsense control for *myc*	ATC CTC CCA ACT TCG ACA TA	20	45	NC
371	Nonsense control for *myc*	TGC CGA GCA CCG GCT TCA TA	20	60	NC
373	Nonsense control for *myc*	TCC ACT TGC C	10	60	NC
62-1	*acpP*	TTC TTC GAT AGT GCT **CAT** AC	20	40	NC
62-2	*acpP*	TC TTC GAT AGT GCT **CAT** A	18	39	NC
62-3	*acpP*	C TTC GAT AGT GCT **CAT**	16	44	NC
62-4	*acpP*	TC GAT AGT GCT **CAT**	14	43	NC
169	*acpP*	C TTC GAT AGT G	11	45	NC
379	*acpP*	TTC GAT AGT G	10	40	NC
380	*acpP*	TTC GAT AGT	9	33	NC
381	*acpP*	TC GAT AGT	8	38	NC
382	*acpP*	TC GAT AG	7	43	NC
383	*acpP*	C GAT AG	6	50	NC
62-5	Nonsense control	TTG TCC TGA ATA TCA CTT CG	20	40	NC
62-7	Nonsense control	G TCC TGA ATG TCA CTT	16	38	NC
62-8	Nonsense control	TCG TGA GTA TCA CT	14	43	NC
170	Nonsense control	TCT CAG ATG GT	11	45	NC
384	Nonsense control	AAT CGG A	7	43	NC

[a] The initiation anticodon is shown in boldface.
[b] That is, the fraction of bases complementary to base-paired, folded mRNA target. NC, not calculated.

the start codon of the gene for firefly luciferase (*luc* from pGL-2; Promega Corp, Madison, Wis.). The constructs were separately transformed into *E. coli* SM101 and AS19.

The acpP-luc reporter (pCNacpP-luc) was made by ligating a SalI-NotI restriction fragment of *luc* with the SalI-NotI fragment of pCiNeo (Promega Corp.), removing the adenosine from the start codon by site-directed mutagenesis, and then directionally cloning a synthetic fragment of *acpP* (bp −17 to +23, inclusive, where +1 is adenosine of the start codon) between the NheI-SalI sites. pCNmyc-luc was made in the same way, except that the *myc* sequence from −14 through +16 (inclusive; numbering adenosine of the start codon as +1) instead of *acpP* was cloned into the NheI-SalI sites. Luciferase enzyme activity was measured in bacteria as described previously (11).

Cell-free protein synthesis. Bacterial cell-free protein synthesis reactions were performed by mixing reactants on ice according to the manufacturer's instruction (Promega Corp.). Reactions were programmed with either pT7myc-luc plasmid in a coupled transcription-translation reaction or mRNA synthesized in a cell-free RNA synthesis reaction (MEGAscript T7 High Yield Transcription Kit; Ambion, Inc., Austin, Tex.) programmed with pT7myc-luc. All acp-luc reactions were programmed with pCNacpP-luc. Where indicated, cell-free reactions were composed with rabbit reticulocyte lysate as described by the manufacturer (Promega Corp.). PMO was added to a final concentration of either 100 or 200 nM as indicated in the figure legends. After 1 h at 37°C, the reactions were cooled on ice and luciferase was measured as described previously (11).

Mammalian tissue culture. HeLa cells were transfected in T75 tissue culture flasks (Nalge Nunc, Inc., Rochester, N.Y.) with a luciferase reporter plasmid (pCNmyc-luc) by using Lipofectamine reagent (Gibco-BRL, Grand Island, N.Y.), according to user's manual, for 5 h in serum-free media (Opti-MEM1; Gibco, Inc., Carlsbad, Calif.) before re-addition of recovery medium (HyQ DME/F-12 supplemented with 20% fetal bovine serum and Gibco Antibiotic-Antimycotic 15240-062; HyClone, Inc., Logan, Utah) at 37°C in 5% CO_2. After 24 h, the cells were pooled, and 10^6 cells were added to each well of a six-well plate (BD Biosciences, San Jose, Calif.) in 2 ml of growth medium. After an additional 24 h, PMO was added to a final concentration of 10 μM in 2 ml of fresh growth medium, and the cells were scraped from the plate surface with a rubber policeman to deliver the PMO to the cells as previously described (22). After scrape loading, the cells were transferred to fresh six-well plates and incubated at 37°C until the time of assay. At 7 and 24 h the cells were examined by microscopy to verify that each culture had the same number of cells, harvested by centrifugation, and lysed in Promega cell culture lysis reagent. Luciferase was measured by mixing the cell lysate with luciferase assay reagent (Promega) and reading the light emission in a model TD-20e luminometer (Turner Designs, Inc., Mountain View, Calif.).

RNA secondary structure. The RNA folding algorithm M-Fold (35) was used to predict the secondary structure of bases 1 to 120 or bases 90 to 1745 of the mRNA transcribed from pT7myc-luc. The folded structure of bases 1 to 120 had a minimum ΔG of −6.5 kcal/mol and that of bases 90 to 1745 had a minimum ΔG of −452.28 kcal/mol. Each PMO was scored (we refer to this as the "2° score") by calculating the fraction of bases (in the PMO) that are complementary to double-stranded (duplex) regions within the folded target mRNA. For example, PMO 331 (Table 1) is 10 bases in length and complementary to a region of myc-luc mRNA that (according to M-Fold) forms duplex RNA at 4 of its 10 bases (the other 6 bases are not paired). The 2° score for PMO 331 would therefore be 4 bases/10 bases, i.e., 0.4.

Statistical analysis. A Spearman rank-order correlation was used to analyze correlations between the inhibitory effects of PMO and either G+C content or secondary structure score of each PMO. An unpaired *t* test (one-sided) was used to analyze differences in inhibition of luciferase, optical density at 600 nm, and CFU/milliliter.

RESULTS

Various PMO lengths. The efficacy of PMO inhibition of target gene expression was tested as a function of the length of PMO. Two series of PMOs (Table 1) were synthesized by sequentially truncating subunits from either the 3′ or 5′ end of a 20-base PMO that is complementary to the region around the start codon of a luciferase reporter gene (*myc-luc*). *myc* is a eukaryotic gene without a similar sequence in *E. coli* and contributes the nontranslated 5′ end and start codon of the reporter transcript. Previous results have shown that the 20-base myc PMO inhibits expression of this reporter gene (11). Each of the various-length (7- to 20-base) PMOs was added to growing cultures of *E. coli* SM101(pSE380myc-luc). After 8 h in culture, luciferase was measured. Compared to a culture without PMO, 3′ truncated PMOs inhibited luciferase from 16 to 95% and 5′ truncated PMOs inhibited luciferase from 6 to 89% (Fig. 1). There is a trend toward more inhibition with shorter PMOs, with a maximum at about nine bases. The seven- and eight-base, 3′ truncated PMOs inhibited less than the same length 5′ truncated PMOs. Control PMOs 371 and 62-8 with nonsense sequences inhibited 0 to 1%. The same pattern of inhibition was found when luciferase was measured at earlier time points (data not shown).

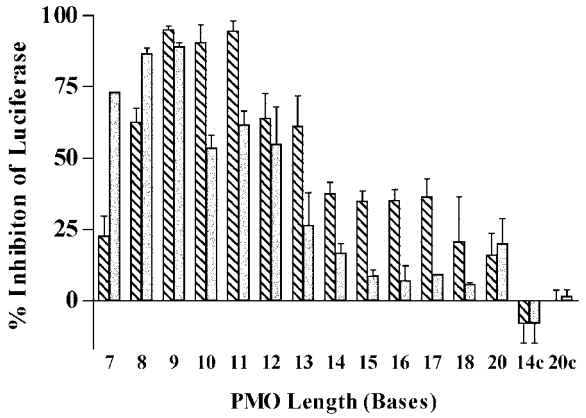

FIG. 1. Effect of PMO length on myc-luciferase expression in *E. coli* SM101. Luciferase activity was measured in cultures of *E. coli* SM101(pSE380myc-luc) grown with various lengths of overlapping PMO (20 μM) targeted to the region around the start codon of *myc-luc*. The percent inhibition was calculated by comparison to a control culture without PMO. Bars: ▨, PMO truncated at the 3′ end (the series from PMO 328 through 126 shown in Table 1); ■, PMOs truncated at the 5′ end (the series from PMO 126 through 334 shown in Table 1). Nonsensical sequence control PMOs (62-8 and 371) are indicated (14c and 20c, respectively). Error bars show the SD (n = 2 to 5).

Cell-free protein synthesis. PMOs from the same two series were added individually to bacterial cell-free protein synthesis reactions programmed to express myc-luciferase. These experiments were designed to eliminate the effects of entry of PMOs into the cell and to test the PMOs at 37°C instead of the permissive growth temperature (30°C) of the conditional mutant SM101. PMOs truncated at the 3′ end from 10 to 20 bases in length inhibited about the same (Fig. 2). Inhibition decreased sharply with 3′ truncated PMOs less than nine bases in length. PMOs truncated at the 5′ end from 12 to 20 bases in length inhibited luciferase about the same (Fig. 2). A sharp decrease in inhibition occurred with 5′ truncated PMOs less than 12 bases in length. Nonsense sequence controls did not inhibit significantly.

Various PMO positions. A series of isometric (10-base) PMOs, which varied by 1 base at each end (Table 1) and was targeted to the region around the AUG start codon of *myc-luc*, was added to bacterial cell-free reactions programmed to synthesize *myc-luc*. All PMOs inhibited luciferase expression (Fig. 3). A trend toward more inhibition was apparent as the target position moved downstream of the start codon. There was no

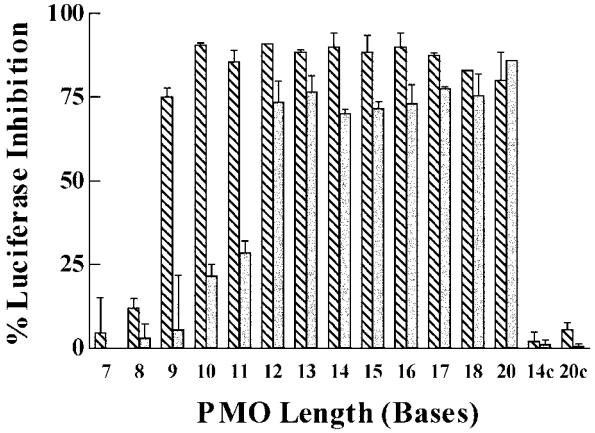

FIG. 2. Effect of PMO length on myc-luciferase expression in cell-free protein synthesis reaction. The same PMOs used for the experiments shown in Fig. 1 were added individually (100 nM) to bacterial cell-free protein synthesis reactions programmed to make myc-luc. After 1 h of synthesis, luciferase was measured. Bars: ▨, 3′ truncated PMOs; ■, 5′ truncated PMOs. Error bars indicate the SD ($n = 2$).

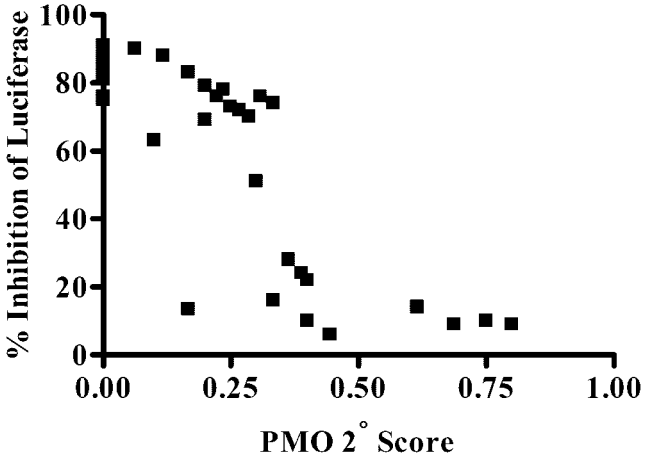

FIG. 4. Correlation analysis. All PMOs targeted to myc-luc (Table 1), except PMOs 214, 215, 327, 328, 333, and 334, were analyzed by comparing the inhibition of luciferase in cell-free reactions with the PMO 2° score (Table 1).

correlation between inhibition and inclusion of the anti-start codon within the PMO sequence.

Another series of PMOs with various lengths was targeted to various positions within the transcript of the *myc-luc*, including the extreme 5′ end of the transcript (PMOs 341 to 344), the ribosome-binding site (PMOs 345 and 347), the region upstream of the ribosome-binding site (PMO 346), the region around and immediately downstream of the start codon (PMO 126), and the 3′ coding region of luciferase (PMOs 214 and 215). Each PMO or a nonsense PMO (371 or 373) was added (200 nM) to a bacterial cell-free protein synthesis reaction programmed to synthesize luciferase. After 1 h at 37°C, luciferase light production was measured. The results were that PMO 126 inhibited luciferase 79%, which was significantly ($P < 0.001$, $n = 4$) more inhibition than that caused by either of the nonsense PMOs 371 or 373 (6 or 4% inhibition, respectively). PMOs 345 and 347 that overlapped the ribosome-binding site inhibited luciferase 24 and 16%, respectively, which for PMO 345 was barely different ($P = 0.016$, $n = 3$) but for PMO 347 was not significantly different ($P = 0.092$, $n = 6$) than the nonsense control PMO 371. Inhibition by each of the other PMOs in this series ranged from 9 to 14% but was not significantly different ($P < 0.1$, $n = 3$ or 5) than either of the nonsense controls.

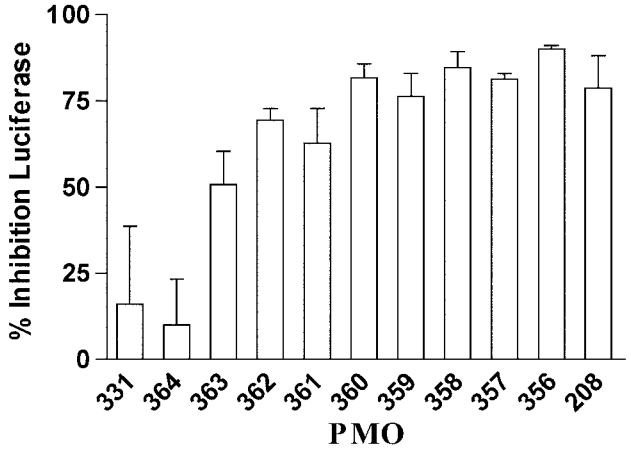

FIG. 3. Effect of PMO position near start codon. Overlapping, isometric (10-base) PMOs, which are complementary to the region around the start codon of *myc-luc*, were added (100 nM) to bacterial, cell-free protein synthesis reactions programmed to make myc-luc. After 1 h of synthesis, luciferase was measured. PMO identification number (Table 1) is shown under each bar. Error bars indicate the SD ($n = 3$).

Statistical analysis of all PMOs targeted to myc-luc, or only the 10-base isometric series indicated no correlation ($r = -0.098$ [$P = 0.54$] and $r = -0.46$ [$P = 0.19$], respectively) between inhibition in the cell-free reactions and percent G+C content. However, an analysis of 37 myc PMOs (Fig. 4), excluding those shorter than nine bases (327, 328, 333, and 334) and those in the 3′ coding region of Luc (214 and 215), revealed a significant negative correlation ($r = -0.85$ [$P < 0.001$]) between inhibition of reporter expression and 2° score of the PMO (Table 1). The 2° score is the fraction of bases in the PMO that are complementary to double-stranded secondary structure within the folded target mRNA (35). An analysis of all 10-base PMOs targeted to *myc-luc* also showed a significant negative correlation ($r = -0.91$ [$P < 0.001$]) between inhibition and 2° score.

PMOs targeted to *acpP*. The effect of PMO was tested on an endogenous bacterial gene, *acpP*, which is essential for viability (34) and has been used previously to inhibit bacterial growth (11, 13). Ten PMOs, which varied in length (6 to 20 bases) and were complementary to the region around the start codon of *acpP* (Table 1), were added to cultures of AS19, and growth at 37°C was monitored by determining the optical density and viable cell counts. Growth curves were normal for all cultures except the one with the 11-base PMO, which grew significantly ($P < 0.001$) slower than the others (Fig. 5A). Viable cells were significantly ($P < 0.001$) reduced at 8 h in cultures grown with a PMO of 10, 11, or 14 bases (Fig. 5B). No reduction in CFU was apparent in cultures treated with a PMO of <10 or more

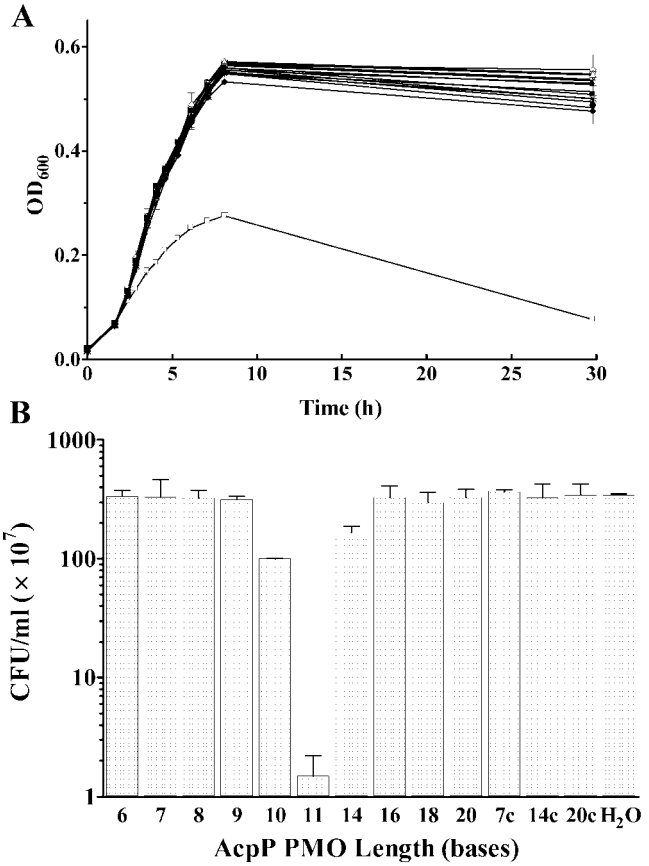

FIG. 5. Effect of AcpP PMO length on growth of *E. coli* AS19. Cultures of *E. coli* AS19 were grown at 37°C with 20 μM PMO (62–1, 62–2, 62–3, 62–4, 169, 379, 380, 381, 382, or 383) of various lengths (6 to 20 bases) and targeted to the region around the start codon of *acpP*. (A) The optical density at 600 nm was monitored over time. The open squares indicate culture with 11-base PMO 169. Nonsense controls included 20 μM PMO 384, 170, 62–8, or 62–5. Error bars indicate the SD ($n = 3$). (B) Viable cells were measured after 8 h. Nonsense base sequence controls included PMOs 384, 62–8, and 62–5. Error bars indicate the SD ($n = 2$ to 7).

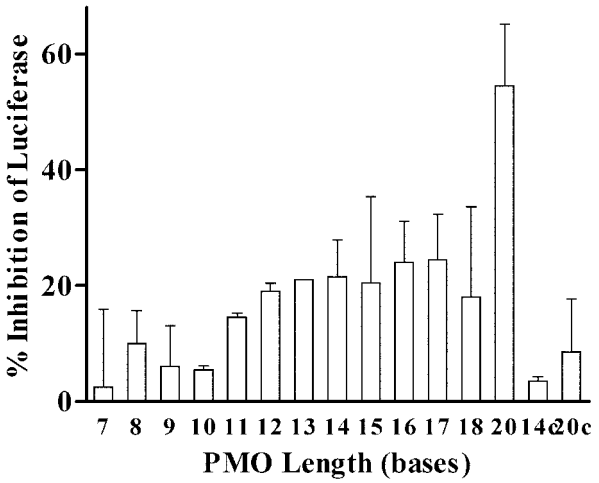

FIG. 6. Reticulocyte cell-free transcription with PMO of various lengths. The same 3′ truncated PMOs used for experiments shown in Fig. 1 were added individually (100 nM) to cell-free protein synthesis reactions composed of reticulocyte lysate and programmed to make myc-luc. After 1 h of synthesis, luciferase was measured. Controls with nonsense sequences (PMOs 62–8 and 62–5) are shown (14c and 20c, respectively). Error bars indicate the SD ($n = 2$).

than 14 bases in length. Cultures without PMO or with one of the variable-length, nonsense base sequence PMOs did not inhibit growth.

Cell-free inhibition of *acpP*. PMOs of various lengths (from 6 to 20 bases) and targeted to *acpP* (PMOs 62-1, 62-2, 62-3, 62-4, 169, and 379 to 383) were added to bacterial, cell-free protein synthesis reactions programmed to express an *acpP-luc* reporter. The results were that PMOs 11 to 20 bases in length significantly ($P < 0.01$, $n = 3$) inhibited reporter expression to about the same extent (ranged from 35 to 50% inhibition). PMOs shorter than 11 bases in length inhibited luciferase expression less than 10% (range, 6 to 9%), which was not significantly ($P > 0.1$) different than nonsense sequence control PMOs 62–5, 62–7, and 384 (1 to 7% inhibition).

PMO effects in HeLa cells. Previous work in eukaryotic systems suggests that PMOs 13 to 14 subunits in length are ineffective (30). We treated HeLa cell cultures that expressed *myc-luc* with 10 μM myc PMO of two lengths (11 and 20 bases [PMOs 340 and 126]). Luciferase was measured at 7 and 24 h after treatment. The results were that at 7 h the 11- and 20-base PMOs inhibited luciferase expression 48% (standard deviation [SD] = 21, $n = 2$) and 58% (SD = 15, $n = 2$), respectively. At 24 h, the longer PMO inhibited luciferase 64% (SD = 6.7, $n = 2$), whereas the shorter PMO inhibited 25% (SD = 7.8, $n = 2$). A culture treated with the nonsense PMO 143 inhibited luciferase nonspecifically 16% (SD = 18, $n = 2$) and 2% (SD = 27, $n = 2$) at 7 and 24 h, respectively.

PMO effects in reticulocyte lysate. The 3′ truncated series of PMOs targeting *myc-luc* were tested for inhibition of luciferase in a cell-free protein translation reaction made with eukaryotic (rabbit reticulocyte) components. The 20-base PMO inhibited significantly more than the shorter PMO (Fig. 6). There was a sharp decrease in inhibition between the 20-base and the 18-base PMO. There was a trend of inhibition that generally favored the longer PMO.

DISCUSSION

Rationales and rules for designing and positioning antisense oligomers within a target mRNA are based on experimental data, theoretical calculations, and bioinformatic screening in eukaryotic systems (8, 18, 15, 28, 30, 32, 33). For PMO and PNA, which inhibit by blocking ribosome function (15), important design considerations include (i) oligomer length and base composition, which affect melting temperature; (ii) target secondary structure, which can interfere with oligomer hybridization; and (iii) position relative to the start codon, which may play a role in blocking ribosome function. Nevertheless, laborious methods of screening remain the rule for designing antisense drugs and identifying target positions (7, 27), particularly in bacteria, which is a relatively new application of antisense drug therapy (13, 21; B. L. Geller, J. Deere, and P. Iversen, submitted for publication).

Some rules for designing antisense antibacterial agents have

recently begun to emerge. For PNA, a length of 10 to 12 bases is optimal (7); however, optimization of PNA length did not correlate with affinity for target (7). Other factors, such as transfer across the outer membrane of *E. coli*, may have accounted for much of the improved efficacy of short PNA. It was not apparent that PMOs as short as 10 to 12 bases would be effective, given the uncertainty of the underlying factors that determined the optimal length of PNA.

We have found that PMOs 9 to 12 bases in length effectively inhibit bacterial gene expression, both in pure culture and in a bacterial cell-free protein expression system. At a reduced temperature of 30°C, PMOs as short as seven bases also caused significant inhibition (Fig. 1), probably because the melting temperature is between 30 and 37°C. The sieving effect of the outer membrane and/or the (unknown) mechanism of transport across the plasma membrane probably accounts for the reduction in efficacy of the longer PMOs (Fig. 1). Indeed, longer PMOs inhibited significantly better in cell-free expression systems than in culture. These results differ from PMO inhibition of eukaryotic gene expression, which is not significant with PMOs less than ~16 bases in length (30). Although the basis for this difference is unknown, we speculate that differences in eukaryotic and prokaryotic ribosome structure, mechanism of subunit assembly on the mRNA, and/or uptake may be important.

Hybridization position of the PMO was also a factor. Recent evidence shows that peptide-PNA inhibited β-lactamase expression only when targeted to either the Shine-Dalgarno sequence (ribosome binding site) or the region around the start codon but not to anywhere else along the entire length of the mRNA (7). Our results show that the region around the start codon is an effective target site. Interestingly, it was not necessary to include the anti-start codon itself within the sequence of the PMO, as exemplified by the inhibition with PMOs 326, 208, or 340 (Fig. 2). In fact, the most effective PMOs that we tested (356, 208, and 169) were targeted slightly downstream of the start codon.

Our results also suggest that the ribosome binding site was a less effective target for PMO inhibition than the region around the start codon, at least for *myc-luc.* The marginal inhibition of *myc-luc* expression by PMOs targeted to the ribosome binding site may suggest that these PMOs poorly block binding of the 30S subunit. This result is different than that shown for peptide-PNA inhibition of expression of β-lactamase or *acpP* (7). Perhaps differences in secondary structures of the three targets, differences in association constants of PNA and PMO, or contributions from the peptide used to facilitate entry of PNA would account for this difference in efficacy at the ribosome binding site.

Other characteristics of PMO were analyzed to detect a correlation with inhibition of *myc-luc*. The G+C content of PMOs did not correlate with inhibition; however, a significant correlation between inhibition and theoretical secondary structure of the targeted region suggests that base pairing within the targeted region may reduce efficacy of the PMO (Fig. 4).

PMOs targeted to sequences far downstream of the AUG start codon did not inhibit expression. This result is consistent with a previous report that showed PNA lack efficacy at downstream sites (7). Each of our downstream PMOs targeted a different predicted secondary structure. One PMO (PMO 215) was targeted to a region predicted to form a stem-like structure with 10 of its 11 bases paired with a contiguous stretch of complementary bases further downstream. The other downstream PMO (PMO 214) was targeted to a region predicted to form a single-stranded region with all 11 of its bases unpaired. Target secondary structure does not appear to be a factor in the lack of efficacy of PMOs targeted to sequences well downstream of the start codon. However, this interpretation relies upon the limitations of secondary structure predictions based on one algorithm.

The efficacy of short (9- to 12-base) PMOs is somewhat unexpected for two reasons. First, in some reports, PMOs shorter than ~16 bases are ineffective in eukaryotic systems (30), whereas in others, PMOs as short as 12 bases cause significant inhibition (15). Second, PMOs have a lower binding affinity than equivalent PNAs and would lose efficacy at a longer length than the equivalent PNA as the length decreased and the T_m fell.

The unexpected efficacy of short PMOs toward bacterial targets prompted us to test them in eukaryotic systems. Although the 20-base PMO was more effective in HeLa cells, the 11-base PMO inhibited target expression. This is consistent with the previous results (15) and shows that a PMO as short as 11 bases can cause a significant target-specific inhibition in eukaryotic cells. However, the 11-base PMO was only marginally effective in the cell-free reticulocyte expression system, whereas the 20 base PMO caused a level of inhibition that was comparable to that found in HeLa cells. This suggests that physiological factors not present in the cell-free reactions favored the shorter PMO in HeLa cells. We speculate that cellular uptake and transport to the cytoplasm likely is the factor that favored the shorter PMO.

ACKNOWLEDGMENTS

We thank Dave Stein and Andrew Kroeker for constructing the reporter plasmids, Rick Bestwick for editorial suggestions, and the Chemistry Department at AVI BioPharma for synthesizing, purifying, and analyzing the PMOs used in these studies.

REFERENCES

1. **Ausubel, F. M., R. Brent, R. E. Kingston, D. D. Moore, J. G. Seidman, J. A. Smith, and K. Struhl.** 1998. Current protocols in molecular biology. John Wiley & Sons, Inc., New York, N.Y.
2. **Bennett, C. F.** 1998. Antisense oligonucleotides: is the glass half full or half empty? Biochem. Pharmacol. **55:**9–19.
3. **Bohnam, M. A., S. Brown, A. L. Boyd, P. H. Brown, D. A. Bruckenstein, J. C. Hanvey, S. A. Thomson, A. Pipe, F. Hassman, J. E. Bisi, B. C. Froehler, M. D. Matteucci, R. Wagner, W. S. A. Noble, and L. E. Babiss.** 1995. An assessment of the antisense properties of RNase H-competent and steric-blocking oligomers. Nucleic Acids Res. **23:**1197–1203.
4. **Borer, P. N.** 1975. Optical properties of nucleic acids, adsorption, and circular dichroism spectra, p. 589. *In* G. D. Fasman (ed.), Handbook of biochemistry and molecular biology: nucleic acids, vol. 1, 3rd ed. CRC Press, Cleveland, Ohio.
5. **Cazenave, C., C. Stein, N. Loreau, N. Thuong, L. Neckers, C. Subashinghe, C. Helene, J. Cohen, and J. Toulme.** 1989. Comparative inhibition of rabbit globin mRNA translation by modified antisense oligodeoxynucleotides. Nucleic Acids Res. **17:**4255–4274.
6. **Dove, A.** 2002. Antisense and sensibility. Nat. Biotechnol. **20:**121–124.
7. **Dryselius, R., S. K. Aswasti, G. K. Rajarao, P. E. Nielsen, and L. Good.** 2003. The translation start codon region is sensitive to antisense PNA inhibition in *Escherichia coli.* Oligonucleotides **13:**427–433.
8. **Far, R. K., W. Nedbal, and G. Sczakiel.** 2001. Concepts to automate the theoretical design of effective antisense oligonucleotides. Bioinformatics **17:** 1058–1061.
9. **Galloway, S., and C. R. H. Raetz.** 1990. A mutant of *Escherichia coli* defective in the first step of endotoxin biosynthesis. J. Biol. Chem. **265:**6394–6402.
10. **Gambacorti-Passerini, C., L. Mologni, C. Bertazzoli, P. Le Coutre, E.**

Marchesi, F. Grignani, and P. E. Nielsen. 1996. In vitro transcription and translation inhibition by anti-promyelocytic leukemia (PML)/retinoic acid receptor alpha and anti-PML peptide nucleic acid. Blood **88:**1411–1417.

11. **Geller, B. L., J. D. Deere, D. A. Stein, A. D. Kroeker, H. M. Moulton, and P. L. Iversen.** 2003. Inhibition of gene expression in *Escherichia coli* by antisense phosphorodiamidate morpholino oligomers. Antimicrob. Agents Chemother. **47:**3233–3239.
12. **Good, L., and P. Nielsen.** 1998. Inhibition of translation and bacterial growth by peptide nucleic acid targeted to ribosomal RNA. Proc. Natl. Acad. Sci. USA **95:**2073–2076.
13. **Good. L., S. K. Awasthi, R. Dryselius, O. Larsson, and P. E. Nielsen.** 2001. Bacterial antisense effects of peptide-PNA conjugates. Nat. Biotechnol. **19:** 360–364.
14. **Hanvey, J. C., N. J. Peffer, J. E. Bisi, S. A. Thomson, R. Cadilla, J. A. Josey, D. J. Ricca, C. F. Hassman, M. A. Bonham, K. G. Au, S. G. Carter, D. A. Bruckenstein, A. L. Boyd, S. A. Noble, and L. E. Babiss.** 1992. Antisense and antigene properties of peptide nucleic acids. Science **258:**1481–1485.
15. **Hudziak, R., J. Summerton, D. Weller, and P. Iversen.** 2000. Antiproliferative effects of steric blocking phosphorodiamidate morpholino antisense agents directed against *c-myc.* Antisense Nucleic Acid Drug Dev. **10:**163–176.
16. **Iversen, P.** 2001. Phosphorodiamidate morpholino oligomers, p. 375–389. *In* Stanley T. Crooke (ed.), Antisense drug technology. Marcel Dekker, Inc., New York, N.Y.
17. **Jayaraman, K., K. McParland, P. Miller, and P. O. Ts'o.** 1981. Selective inhibition of *Escherichia coli* protein synthesis and growth by nonionic oligonucleotides complementary to the 3′ end of 16S rRNA. Proc. Natl. Acad. Sci. USA **78:**1537–1541.
18. **Knudsen, H., and P. E. Nielsen.** 1996. Antisense properties of duplex- and triplex-forming PNA. Nucleic Acids Res. **24:**494–500.
19. **Marcus-Sekura, C. J., A. M. Woerner, K. Shinozuka, G. Zon, and G. V. Quinnan, Jr.** 1987. Comparative inhibition of chloramphenicol acetyltransferase gene expression by antisense oligonucleotide analogues having alkyl phosphotriester, methylphosphonate, and phosphorothioate linkages. Nucleic Acids Res. **15:**5749–5763.
20. **Mologni, L., P. Le Coutre, P. E. Nielsen, and C. Gambacorti-Passerini.** 1998. Additive antisense effects of different PNA on the in vitro translation of the PML/RARα gene. Nucleic Acids Res. **26:**1934–1938.
21. **Nielsen, P. E.** 2000. Peptide nucleic acids: on the road to new gene therapeutic drugs. Pharmacol. Toxicol. **86:**3–7.
22. **Partridge, M., A. Vincent, P. Mathews, J. Puma, D. Stein, and J. Summerton.** 1996. A simple method for delivering morpholino antisense oligos into the cytoplasm of cells. Antisense Nucleic Acid Drug Dev. **6:**169–175.
23. **Pooga, M., U. Soomets, M. Hallbink, A. Valkna, K. Saar, K. Rezaei, U. Kahl, J.-X. Hao, X.-J. Xu, Z. Wiesenfeld-Hallin, T. Hokfelt, T. Bartfai, and U. Langel.** 1998. Cell penetrating PNA constructs regulate galanin receptor levels and modify pain transmission in vivo. Nat. Biotechnol. **16:**857–861.
24. **Rahman, M. A., J. Summerton, E. Foster, K. Cunningham, E. Stirchak, D. Weller, and H. W. Schaup.** 1991. Antibacterial activity and inhibition of protein synthesis in *Escherichia coli* by antisense DNA analogs. Antisense Res. Dev. **1:**319–327.
25. **Rapaport, E., A. Levina, V. Metelev, and P. C. Zamecnik.** 1996. Antimycobacterial activities of antisense oligodeoxynucleotide phosphorothioates in drug-resistant strains. Proc. Natl. Acad. Sci. USA **93:**709–713.
26. **Sekiguchi, M., and S. Lida.** 1967. Mutants of *Escherichia coli* permeable to actinomycin. Proc. Natl. Acad. Sci. USA **58:**2315–2320.
27. **Sohail, M., H. Hochegger, A. Klotzbucher, R. L. Guellec, T. Hunt, and E. M. Southern.** 2001. Antisense oligonucleotides selected by hybridization to scanning arrays are effective reagents in vivo. Nucleic Acids Res. **29:**2041–2051.
28. **Stein, D., E. Foster, S.-B. Huang, D. Weller, and J. Summerton.** 1997. A specificity comparison of four antisense types: morpholino, 2′-*O*-methyl RNA, DNA, and phosphorothioate DNA. Antisense Nucleic Acid Drug Dev. **7:**151–157.
29. **Summerton, J., and D. Weller.** 1997. Morpholino antisense oligomers: design, preparation, and properties. Antisense Nucleic Acid Drug Dev. **7:**187–195.
30. **Summerton, J.** 1999. Morpholino antisense oligomers: the case for an RNase H-independent structural type. Biochim. Biophys. Acta **1489:**141–158.
31. **Wagner, R. W., M. D. Matteucci, D. Grant, T. Huang, and B. C. Froehler.** 1996. Potent and selective inhibition of gene expression by an antisense heptanucleotide. Nat. Biotechnol. **14:**840–844.
32. **Walder, R., and J. Walder.** 1988. Role of RNase in hybrid-arrested translation by antisense oligonucleotides. Proc. Natl. Acad. Sci. USA **85:**5011–5015.
33. **White, D. G., K. Maneewannakul, E. von Hofe, M. Zillman, W. Eisenberg, A. K. Field, and S. B. Levy.** 1997. Inhibition of the multiple antibiotic resistance (*mar*) operon in *Escherichia coli* by antisense DNA analogs. Antimicrob. Agents Chemother. **41:**2699–2704.
34. **Zhang, Y., and J. E. Cronan, Jr.** 1996. Polar allele duplication for transcriptional analysis of consecutive essential genes: application to a cluster of *Escherichia coli* fatty acid biosynthetic genes. J. Bacteriol. **178:**3614–3620.
35. **Zuker, M.** 2003. M fold web server for nucleic acid folding and hybridization prediction. Nucleic Acids Res. **31:**3406–3415.